Spatial calibration of the EO-1 Advanced Land Imager

David R. Hearn , Jeffrey A. Mendenhall, and Berton C. Willard

MIT Lincoln Laboratory
244 Wood Street, Lexington, MA 02420-9185

ABSTRACT

Spatial calibrations have been performed on the Advanced Land Imager (ALI) of the EO-1 satellite. Topics discussed in this paper include end-to-end imaging tests, measurements of system modulation transfer function (MTF), and pixel lines of sight. The MTF measurements were made by recording scans of a knife-edge past the pixels. The techniques used to place the focal plane at the correct focal position are described, since they make use of MTF measurements. Line-of-sight (LOS) measurements combine theodolite measurements of the telescope distortions and the photolithographic patterns of the detector arrays with images of a stationary Ronchi ruling recorded with the instrument at its normal operating conditions in a thermal vacuum chamber.

Keywords: calibration, EO-1, MTF, thermal/vacuum

1. INTRODUCTION

The Advanced Land Imager (ALI) of the EO-1 satellite has been described by Digenis, et al.[1] General descriptions of the calibration of this instrument have been given in several papers.[2,3,4] The preflight calibrations have now been completed. They consisted of radiometric, spectral, and spatial calibration phases, which employed different equipment setups. This paper describes the spatial calibrations. The following sections cover the measurement setup and equipment, end-to-end imaging tests, modulation transfer function measurements, focus adjustment, and pixel line-of-sight measurements. Examples of the resulting calibration information are shown.

2. MEASUREMENT SETUP

All testing and calibration of the ALI was carried out in a Class 1,000 clean room at Lincoln Laboratory. Within the clean room, the ALI was kept either in a thermal vacuum chamber or under a class 100 clean hood. These precautions were taken to avoid contamination of the optical surfaces. Most of the computers ancillary to the calibration and testing process were located in an anteroom to the clean room.

2.1. Imaging Collimator

All of the spatial calibrations employed an imaging collimator, which had to satisfy several demanding requirements. It had to have diffraction-limited performance over a 3.2¡ field of view (FOV). In addition, the unobscured exit pupil had to be several meters away from the collimator, so that it could be placed in coincidence with the virtual entrance pupil of the ALI instrument. These requirements were met by a wide-FOV Schmidt-sphere imaging collimator, which is fully described by Willard.[5] The methods used to establish the collimation of the output beam are also described in that reference. A layout of the collimator bench is shown in Figure 1. The light source is a 250 W quartz tungsten halogen lamp, with a 6-inch integrating sphere behind the condensing lens. The exit port of the integrating sphere forms the pupil of the collimator, in order to illuminate the ALI entrance pupil uniformly.

This work was sponsored by NASA/Goddard Space Flight Center under U. S. Air Force Contract F19628-95-C-0002.

Opinions, interpretations, conclusions, and recommendations are those of the author and are not necessarily endorsed by the United States Air Force.

Correspondence: Email: drhearn@ll.mit.edu; Telephone: 781-981-0918; Fax: 781-981-4608

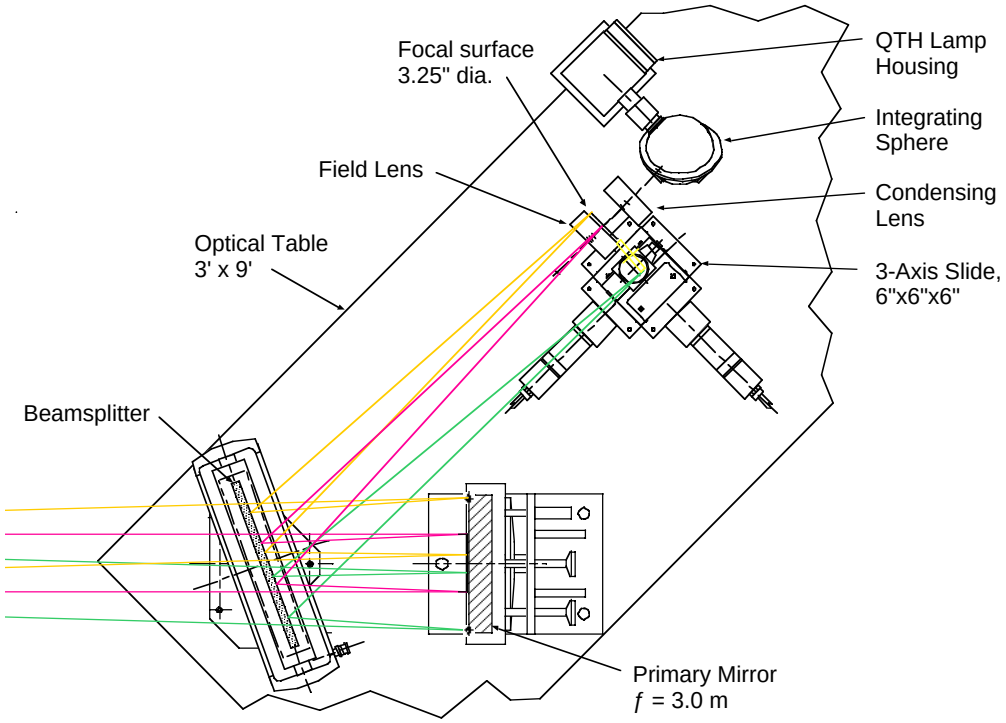

Figure 1. Top view of the imaging collimator used for spatial calibrations of the ALI. Overall dimensions of the table are 3x9 feet.

At the focal plane of the collimator were placed various target masks for testing the response of the ALI. These targets were mounted on a three-axis linear stage so that they could be translated under computer control. Horizontal motions were provided by two Aerotech model ATS 1500 stages, with 152 mm travel ranges. A Klinger model MT160 stage gave the vertical motion, over a 150 mm range. In addition, two Newport slides with model 850 motor drives were used for more precise scan motions in the focal plane over ranges of less than 10 mm. This was necessary because interferometric measurements of the motions of the long-stroke slides had shown that errors in their lead screws were unacceptably large, despite the 1 m precision of their micro-stepping drives.

2.2. Control and Data Acquisition System

All equipment that had to be controlled in real time was interfaced with the ALI Calibration Control Node (ACCN) computer next to the collimator bench, operating under Windows NT. The control software on that machine was LabVIEW. An Ethernet backbone connected the ACCN with the Electrical Ground Support Equipment computer number 1 (EGSE1) and the Performance Assessment Machine (PAM). The EGSE1 is a Sun workstation with special data-acquisition boards, and the PAM is a Silicon graphics R-10000, running unix. Focal plane data from the ALI were received by the EGSE1, then transferred to the PAM. Quick-look processing was carried out on the PAM. The results were displayed on a monitor in the clean room, next to the ACCN, to verify that adequate data had been collected. All data were stored on a hard-disk array, and archived on digital linear tape (DLT) cartridges.

2.3. Support Fixture

When the ALI was not mounted in the thermal vacuum chamber, it was supported on a handling fixture made by Flotron. This fixture provides a horizontal rotation axis for the plate that carried the ALI. Large castors permit the fixture to be moved around easily. Since some of the optical testing was to be done while the ALI was on this fixture, special vertical jacks were added to support the fixture rigidly from the floor. Also, clamping collars were made, to prevent unwanted motions of the vertical adjustment tubes of the Flotron fixture. No discernable vibration of the instrument occurred while optical measurements were being made with this setup.

2.4. Thermal Vacuum Chamber

Most calibration measurements on the ALI were performed while the instrument was in the thermal vacuum chamber. The short-wave infrared (SWIR) detectors of the ALI could not be tested otherwise. This chamber includes a liquid-nitrogen cooled shroud, which was maintained around 100 K. The inside dimensions of the shroud are approximately 1.78 m in diameter by 1.52 m deep. The pressure in the chamber during the calibrations of the ALI ranged from 10^{-7} to 10^{-11} Torr.

Centered in the end door of the horizontal chamber is a fused-silica window, with a clear aperture of 30.5 cm (12 inches). The window had previously been dismounted and characterized for transmitted wavefront error and spectral transmission. The beam of the collimator was directed through this window.

2.5. Azimuth Positioning System

The virtual entrance pupil of the ALI is 0.54 m behind the mounting face of the instrument pallet. It was necessary to be able to rotate the ALI about the center of the entrance pupil in order to carry out all of the various tests to be performed in the vacuum chamber. Accordingly, a motorized fixture was built, to enable the ALI to be rotated about a vertical axis through its pupil. The X (line of flight) axis of the ALI pointed down while mounted on this fixture. Thus, the entire 15¡ cross-track FOV of the instrument could be accessed with the fixed collimator beam.

2.6. Window Measurement Setup

After the focus shim of the ALI had been adjusted, the instrument was placed on the azimuth stage in the vacuum chamber. Focus tests were again made on the ALI, before and after the chamber door was closed, and after the chamber was evacuated. No shift in apparent focus was observed. However, when the shroud was cooled to bring the instrument to its normal operating temperature, the next focus tests showed a change of ~150 m in the apparent position of the focal plane. This was due to a radial gradient in the index of refraction of the chamber window, caused by radiative cooling of the window by the cold shroud. A Fizeau interferometer, Zygo Mark IV, was set up to measure the interference fringes formed between the front and back faces of the window. A 12-inch diameter flat mirror was manually inserted in the collimator beam to direct the Zygo toward the window prior to each imaging calibration session. The Zygo then analyzed and displayed the apparent optical power of the window. A small offset was added to the focal position of the collimator in order to compensate for the opto-thermal window power. Hearn gives a fuller description and analysis of this window phenomenon.[6]

3. END-TO-END IMAGING TEST

Starting as soon as the focal plane detection system was integrated with the instrument, end-to-end imaging tests were performed. In these tests, the target in the collimator was translated vertically at the correct speed to simulate the apparent ground motion from the satellite. The entire multispectral array, of 3¡ cross-track extent, thus scanned a simulated earth scene. Offset and gain corrections were applied to the pixel data. The image in each band was reconstructed in the PAM, and the results were displayed and printed. These tests were performed in order to verify the basic operation of the focal plane system and the reconstruction software, as well as to check for more subtle image artifacts.

The principal target pattern employed for the end-to-end imaging tests was a USAF 1951 target, with a clear pattern on chrome (black) background (Edmund Scientific No. H36408). An example of a reconstructed image of this target is shown in Figure 2. Other targets used included color photographic transparencies, and a leaf in fall color, sandwiched between glass plates.

These tests soon revealed that two of the pixels (out of 15,360) of the focal plane array (FPA) were cross-coupled to some of the other pixels of the same band. It appears that this leaky pixel effect can be compensated, with suitable modifications in the radiometric calibration pipeline software.

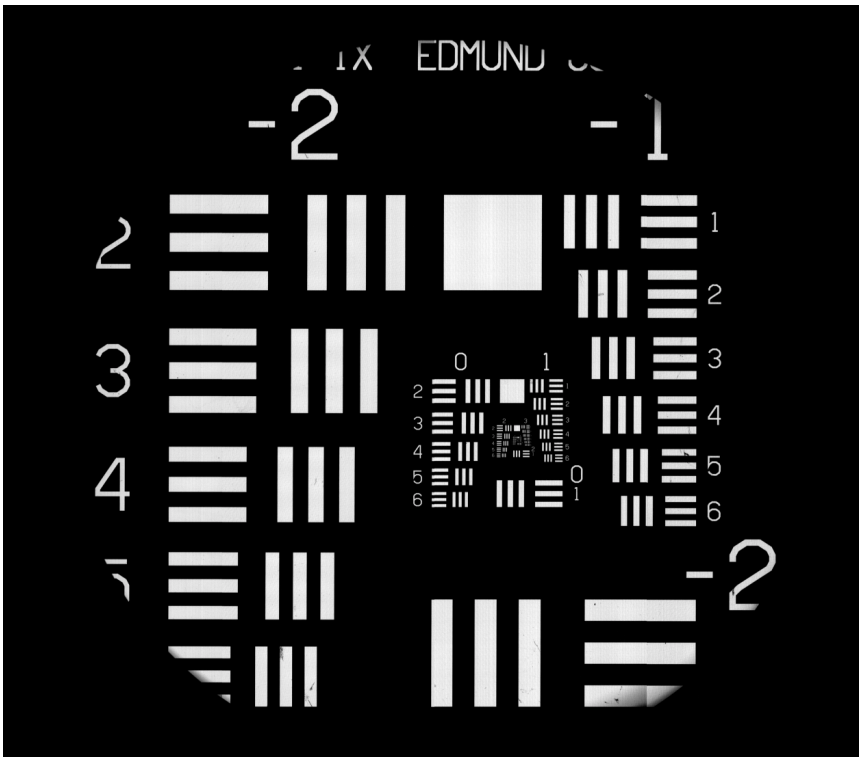

Figure 2. Reconstructed image of the USAF 1951 target, as acquired by the ALI through the imaging collimator. Offset and gain corrections have been applied to the pixel readings.

4. MODULATION TRANSFER FUNCTION TESTS

The most comprehensive measure of optical resolution in an imaging system is its system modulation transfer function (MTF). It can be defined as the Fourier transform of the system point-spread function (PSF). Since a Fourier transform is in general complex, the MTF is often defined as the *magnitude* of the transform, and a phase transfer function (PTF) is then used to complete the description.[7] We prefer to treat the MTF as a complex function in the present application. If the PSF is symmetrical about its origin, the MTF is real. Asymmetry in the PSF is manifested by a non-zero imaginary part of the MTF. (Since the PSF is real, the real part of the MTF is always symmetric, and the imaginary part is anti-symmetric.) If an imaging system provides a high signal-to-noise ratio, and its MTF is well enough characterized, it is possible, through the use of the MTF, to enhance the resolution of the images it produces.

The MTF is a two-dimensional function of spatial (or angular) frequency orthogonal to the viewing axis. It can also be a function of the position within the field of view of the instrument, making it actually four-dimensional. At any given point in the field, the optical transfer function is the autocorrelation of the optical amplitude within the system pupil (with suitable scaling factors). Wavefront errors of the ALI telescope were characterized at eleven field points by SSG, which built the telescope. They analyzed interferograms obtained with a laser unequal-path interferometer (LUPI), and described the wavefront errors by a set of 37 Zernike polynomial coefficients at each field point. We have developed software to interpolate those coefficients at any part of the FOV, and reconstruct the ALI wavefronts. The squared magnitude of the Fourier transform of the complex amplitude within the pupil is the computed PSF. The optical MTF is then the Fourier transform of the PSF. Examples of these computed functions are shown in Figures 3 to 5.

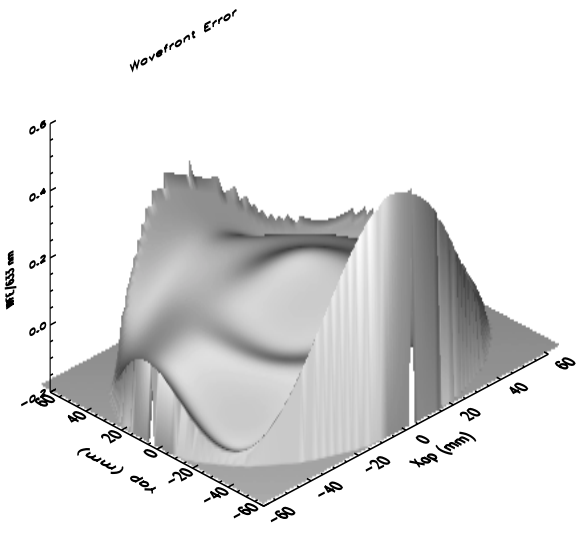

Figure 3. Wavefront error near the center of the MS/Pan array, reconstructed from LUPI interferograms. No focus term is included.

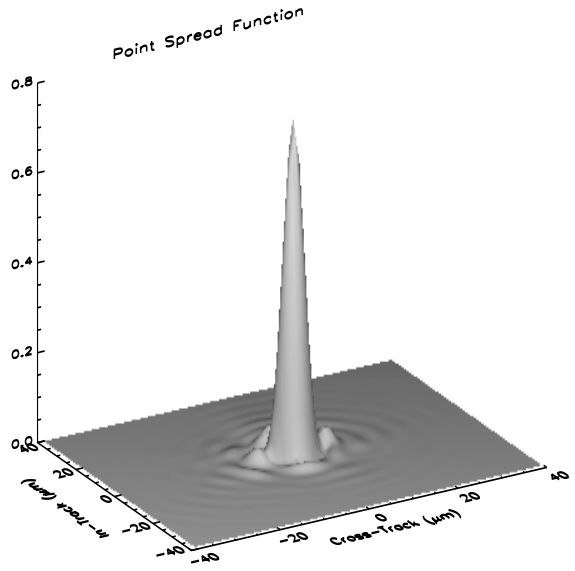

Figure 4. Point spread function for Pan band near the center of the MS/Pan array, computed from the wavefront error shown in Figure 3. (No focus error.)

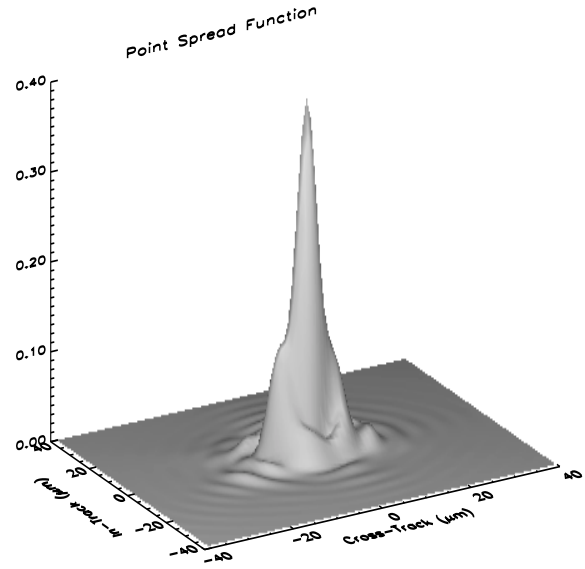

Figure 5. Point spread function as in figure 4, but with 119˚ m focus error at the FPA.

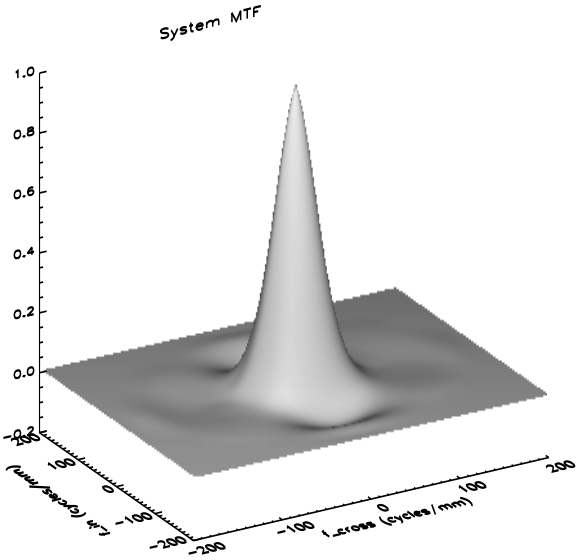

Figure 6. System MTF of the ALI Pan band, as derived from interferogram measurements. (With 119 m focus error.)

The pixel detectors of the ALI are 13.2 m square for the panchromatic (Pan) band, and 39.6 by 40 m for the multispectral (MS) bands. The detectors are expected to respond uniformly across these respective active areas. The MTF of each pixel is thus a product of two sinc functions, running in the cross-track and in-track directions. When the optical MTF is multiplied by the pixel MTF, the result is a system MTF, as shown in Figure 6.

To measure the system MTF s of the ALI, knife-edge scans were made across representative pixels of each band and each sensor chip assembly (SCA), in both cross-track and in-track directions. The knife-edge employed was the horizontal or vertical side of the open 9 mm square of the USAF 1951 target. During these scans, other parts of the target were covered by a mask. The scans were done by translating one of the Newport slides at 200 m/s while recording focal plane data. The apparent speed of the edge was 127 m/s at the ALI focal plane. Since the MS frame rate was set at 226 frames/s, the spatial sampling rate was 1,774 samples/mm at the ALI focal plane. For the Pan band, the frame rate is three times higher, so the spatial sampling rate was 5,322 samples/mm.

The detected signals, when normalized to a response range of zero (black) to one (white), represent the edge-spread function (ESF) of each pixel. A fit was performed on each pixel ESF in order to center them to a common origin. The derivative of the ESF is the line-spread function (LSF). The differentiation was performed in the Fourier transform domain, where a low-pass filter was easily applied to suppress noise beyond the diffraction cutoff. The mean LSF was then computed. Each pixel LSF was Fourier transformed to obtain the individual MTF s. Finally, the MTF s were averaged to find the mean MTF for that band, SCA, and scan direction. Representative samples of these various functions are plotted in Figures 7 through 10.

Since a knife-edge scan can only be used to estimate a line-spread function, not a point-spread function, the MTF s derived from these scans actually represent one-dimensional slices through the (two-dimensional) MTF, through the origin in a direction perpendicular to the edge. An estimate of the full, two-dimensional MTF may be obtained by comparison of the measured MTF s obtained from the knife-edge scans with those calculated from the interferogram data. It is necessary to adjust the three parameters describing the position of the FPA in the focus direction until the best match is found between the measured and the calculated MTF s. This has been done, and the system MTF estimate for Band 4 is shown as a two-dimensional function in Figure 11.

Although the knife-edge scan technique used for this instrument is applicable to sparse arrays of pixels, and can produce an estimate of the MTF for all frequencies to the diffraction cutoff, it can be compromised by practical limitations. Optical turbulence and mechanical jitter of the system must be held to a minimum. Irregular motions of the scanning slides were the greatest problem in this instance. Taking averages over many pixels, and skewing the knife edge at a small angle to the rows of pixels alleviated this difficulty for most of the scans performed on the ALI.

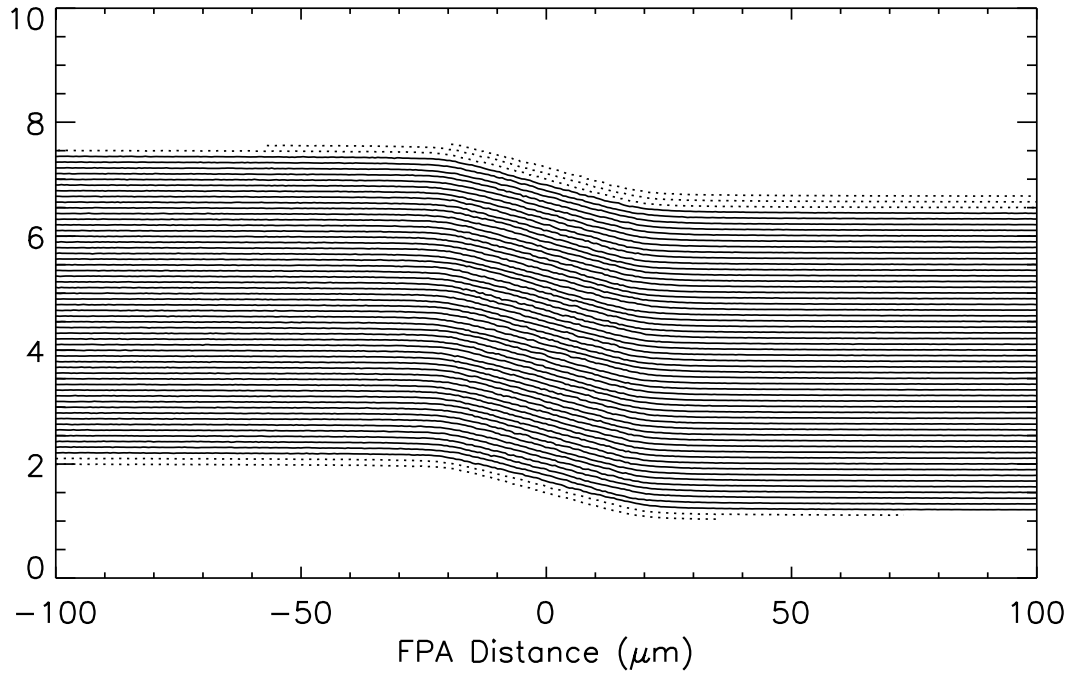

Figure 7. Edge-spread functions for Band 4, SCA 2, cross-track direction. The dotted curves are for pixels which were not used in further analyses, because of artifacts in their scan data.

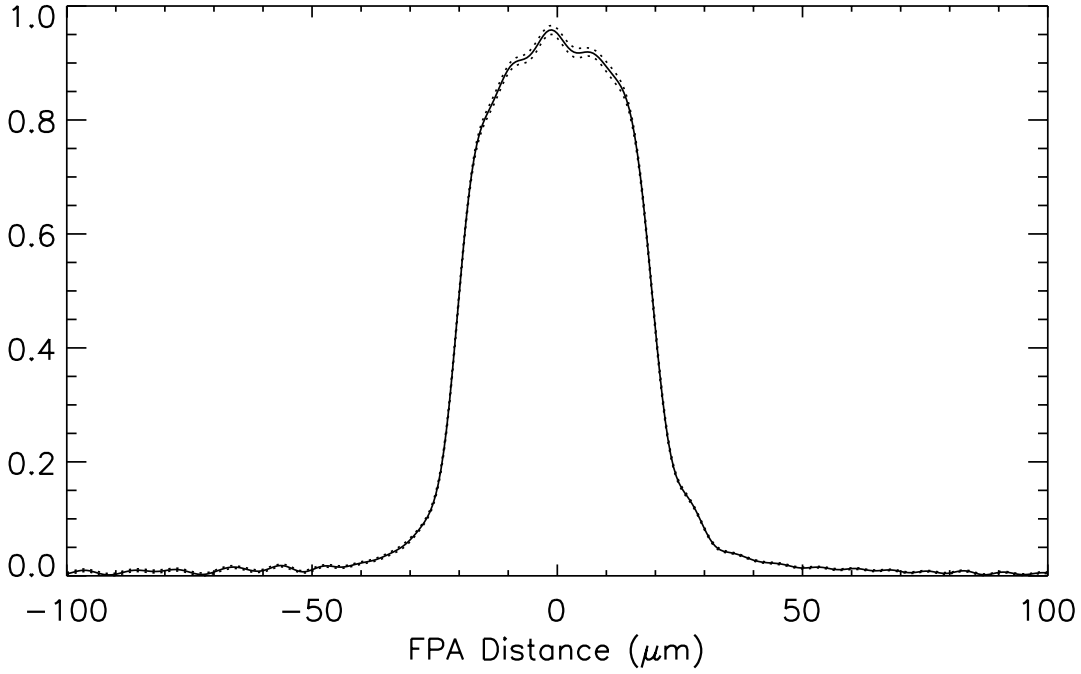

Figure 8. Average line-spread function for the scan shown in Figure 7. The dotted curves are one standard deviation above and below the mean.

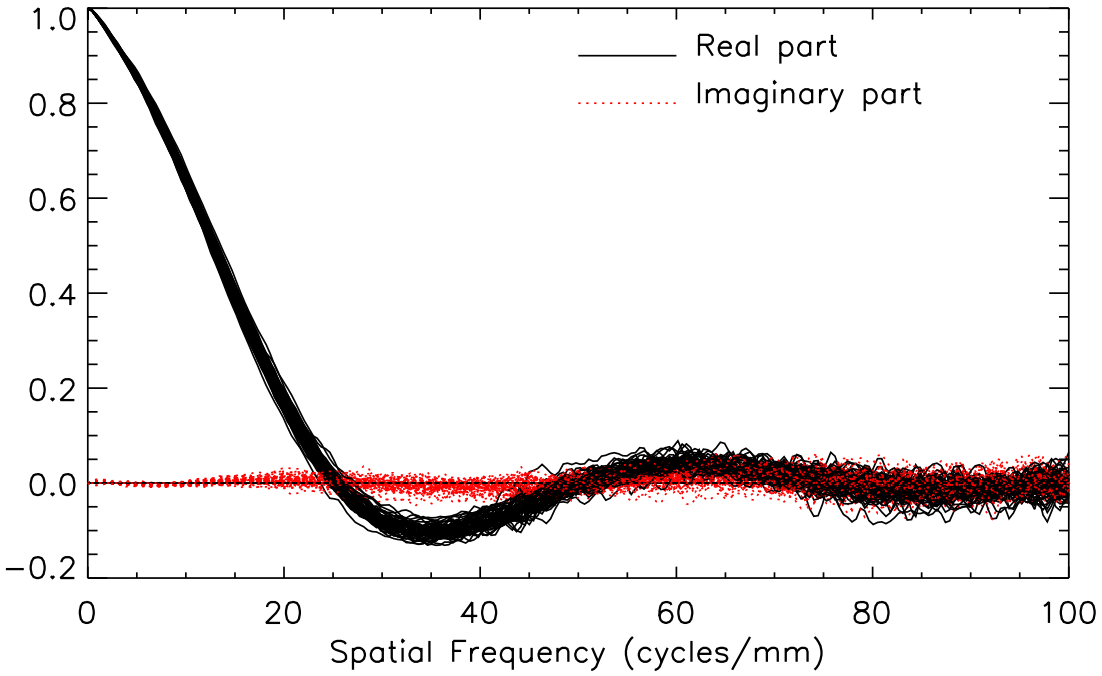

Figure 9. Individual pixel MTF curves for the scan shown in Figure 7.

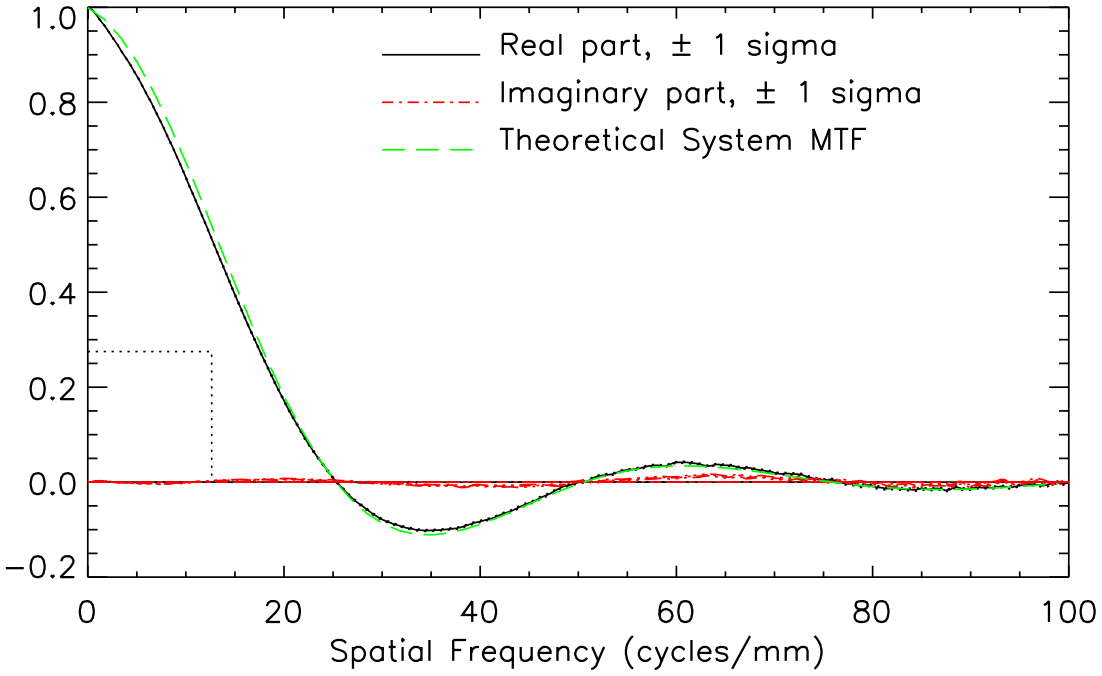

Figure 10. Average MTF for the scan shown in Figure 7, with one standard deviation limits also shown. The curve in long dashes is the corresponding MTF calculated from the optical interferograms and the assumed geometry of the detectors. For reference, the MTF value specified at the Nyquist frequency, 12.63 cycles/mm, is also plotted (dotted lines).

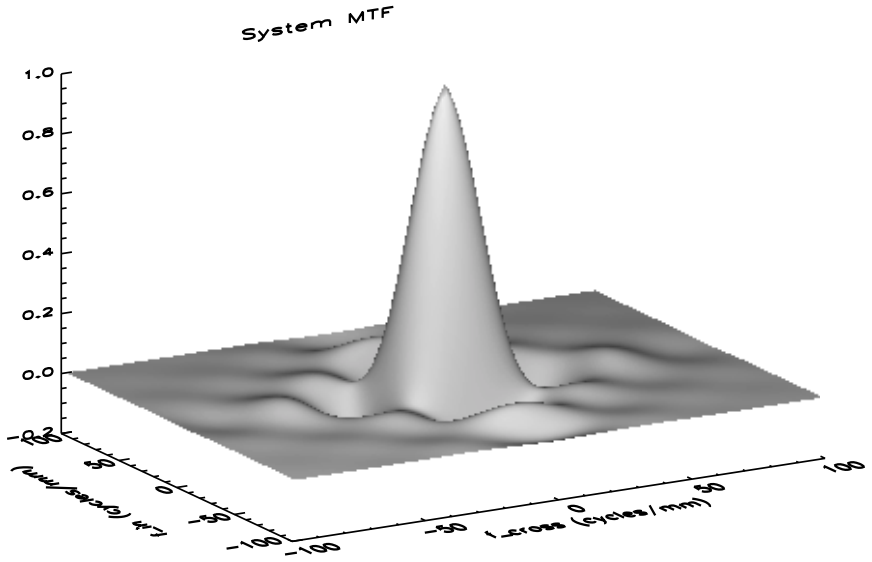

Figure 11. Estimated two-dimensional system MTF for Band 4.

5. FOCUS MEASUREMENT AND ADJUSTMENT

One of the early steps in the integration of the ALI focal plane system with the telescope was to establish the proper thickness for the shim which would place the FPA at the best-focus plane of the telescope. The necessary measurements were made while the ALI was mounted on the Flotron fixture, and only the visible detectors were used. An iterative procedure was planned, based on measurements of the system MTF, as described in the preceding section. Successive knife-edge scans were made, with the plane of the knife-edge displaced by various distances from the true collimator focus position. For each scan, a figure-of-merit was calculated, indicating the relative quality of the focus. This was either the integral of the MTF from zero to some fixed frequency (such as the ALI sampling frequency), or the inverse slope of the middle portion of the ESF. The figures of merit were plotted, and the position of the knife-edge was found which gave the best focus. The distance of that position from the true collimator focus, when multiplied by the square of the ratio of focal lengths (ALI telescope to collimator), was the estimated focus error in the ALI. The FPA was then removed, the shim was corrected, and the process was repeated. In this case, only one cycle of shim adjustment was made.

6. LINE-OF-SIGHT MEASUREMENTS

The line-of-sight (LOS) measurements were done in two phases, which may be categorized as relative and absolute. The relative measurements are to estimate the LOS of each pixel relative to all of the rest of the pixels. Optical distortions in the telescope and inaccuracies in the placement of the SCA s affect these relative lines of sight. Absolute measurements are needed to relate the ALI LOS to the inertial reference unit of the spacecraft, and to the other instruments on board. The absolute measurements relate the pixels to an optical reference cube mounted on the pallet of the ALI, next to the telescope housing.

Two methods were used to estimate the relative pixel lines of sight. First, subsystem measurements were made, on the telescope and focal plane separately. Second, measurements were made with the integrated system. The subsystem measurements by Santa Barbara Remote Sensing (SBRS) on the assembled focal plane used a coordinate-measuring machine to establish the locations of fiducial marks in the metallization of each SCA, to an accuracy of ~ – 1 m. The location of the pixels within each SCA, determined by photolithography, was assumed to have a precision of ~ – 0.1 m. To characterize the telescope distortion, a fixture bearing scribed lines was mounted at the focal plane location. These lines were also measured

on a coordinate-measuring machine. A precision theodolite was then used by SSG to measure the angles of the scribe-line intersections when seen through the telescope, to – 1 arc sec. These angular readings were then fitted to cubic polynomial functions to describe the cross-track and in-track optical distortion. Vector maps of the measured distortions, and the residuals from the fits are shown in Figures 12 and 13.

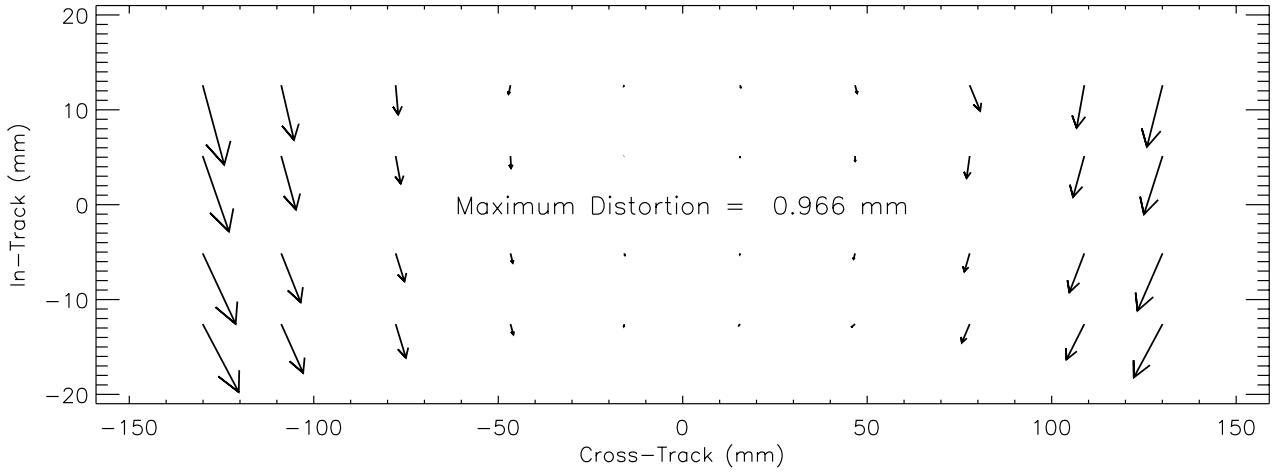

Figure 12. ALI telescope optical distortion, from SSG measurement data. The axes encompass the entire 15¡x1.2¡ field of view of the telescope. The longest vector represents 0.966 mm of distortion at the focal plane.

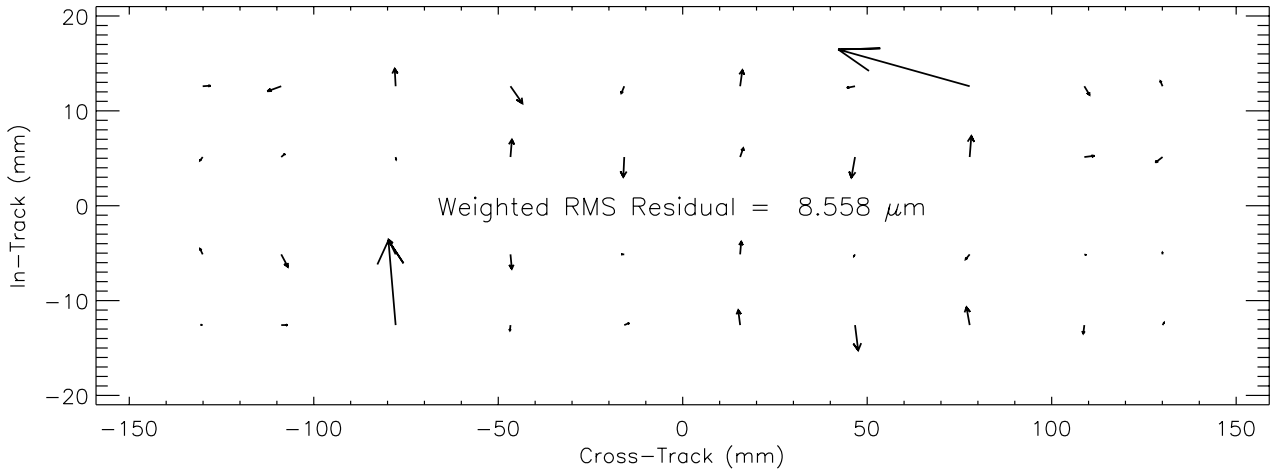

Figure 13. Residual ALI optical distortion, after subtracting a cubic polynomial fit from the measurement data. The fitted focal lengths are 942.41 mm and 945.15 mm in the cross-track and in-track directions, respectively. The scale of the vectors is greatly enlarged in comparison with Figure 12. (The 8.6 m rms residual value does not include the two largest residuals, which are probably the results of erroneous data.)

The relative line-of-sight measurements of the integrated system were done by using a large Ronchi ruling as the target in the imaging collimator. A small bulls-eye was added to the target to mark the axis of the collimator, which has some distortion of its own. The ruling has a frequency of 2.0 cycles/mm. Static images were acquired by the ALI, with the ruling lines oriented at 0¡, 60¡, and 120¡. (A scanned image of the ruling, acquired in the same setup, is shown in Figure 14.) A multi-parameter fit was then performed on the three static images, to obtain the set of parameter values to describe the relative pixel lines of sight.

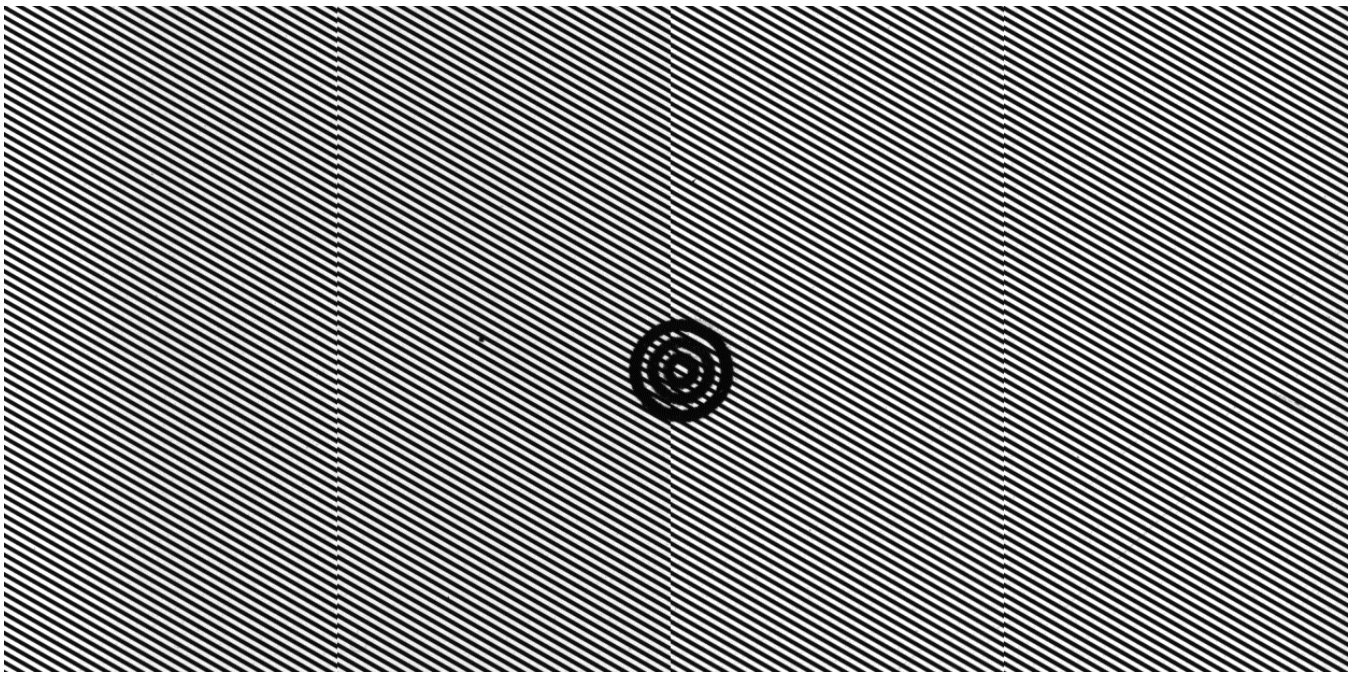

Figure 14. Scanned ALI image of the Ronchi ruling used for pixel LOS determination.

Absolute LOS measurements were made with the ALI on the Flotron fixture, with its optical axis horizontal. An electronic, auto-leveling precision theodolite, Zeiss Model Eth 2, was used to measure the azimuth and elevation of the normal to each visible face of the reference cube, by autocollimation. A 12-inch flat mirror on a fixed stand served as the azimuth reference. Using the same references, the theodolite was positioned to view the pixels of the focal plane, directly through the ALI telescope. At 30 power, the observers were able to resolve features in the metallization that delineated the ends of the Pan band array on each SCA. For this observation, two Mag Lite flashlights, supported on each side of the theodolite, provided adequate illumination. The appearance of the FPA was strongly dependent on the position and angle of the light source, however. All of the azimuth and elevation readings were converted to vectors. The vectors were then rotated to express them in a coordinate system defined by the reference cube. In the course of this process, it was verified that the operative cube faces are orthogonal to within 7 arc sec.

7. IN-FLIGHT TESTS

Data taken with the ALI in flight will be used to verify its performance. Long, linear features of high contrast will be imaged, to check the MTF performance. Lunar calibrations, in which the ALI is slowly scanned across the moon, will yield the best in-flight test of MTF. Well-known Ground Control Points will be used to validate the pixel LOS parameters, especially the overall relationship to the on-board inertial reference system. Band-to-band registrations within the images will be verified.

8. ACKNOWLEDGEMENTS

Many individuals contributed to the success of the present calibrations. The authors wish to thank especially Vincent Cerrati, Herb Feinstein, and Travis Hein of Lincoln Laboratory for essential engineering support. Vicki Loriaux, Brian Norman, and Gerry Perron of SSG produced optical data on the telescope. Cliff Nichols and Paul Bryant, of SBRS, provided the SCA position measurements.

9. REFERENCES

1. Digenis, C. J., Lencioni, D. E., and Bicknell, W. E., “New Millennium Advanced Land Imager,” Proc. SPIE, Vol. 3439, pp.49-55, July 1998.

2. Mendenhall, J. A., Lencioni, D. E., Hearn, D. R., and Parker, A. C., “EO-1 Advanced Land Imager preflight calibration,” Proc. SPIE, Vol. 3439, pp.390-399, July 1998.

3. Mendenhall, J. A., Lencioni, D. E., Hearn, D. R., and Parker, A. C., “EO-1 Advanced Land Imager in-flight calibration,” Proc. SPIE, Vol. 3439, pp.416-422, July 1998.

4. Lencioni, D. E., Hearn, D. R., Mendenhall, J. A., and Bicknell, W. E., “EO-1 Advanced Land Imager calibration and performance overview,” This conference, paper number [3750-12].

5. Willard, B. C., “Wide field-of-view Schmidt-sphere imaging collimator,” This conference, paper number [3750-36].

6. Hearn, D. R., “Vacuum window optical power induced by temperature gradients,” This conference, paper number [3750–37].

7. Holst, G. C., *Electro-Optical Imaging System Performance*, SPIE Press, 1995.